



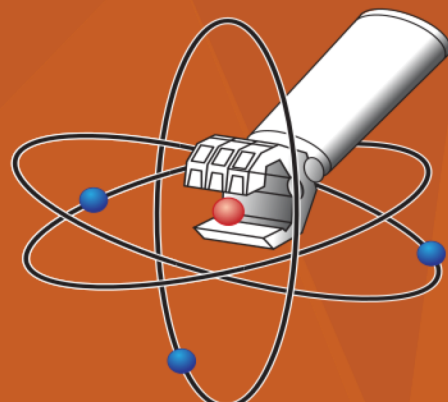
The University of Texas at Austin
WHAT STARTS HERE CHANGES THE WORLD

Control and Path Planning of a Wheeled Mobile Robot with Centered Orientable Wheels and an Offset Sensor for Radiation Surveying Applications

Honors Thesis Symposium

Vikram Ramanathan
B.S. Mech. Engineering, May 2020

N
R
G

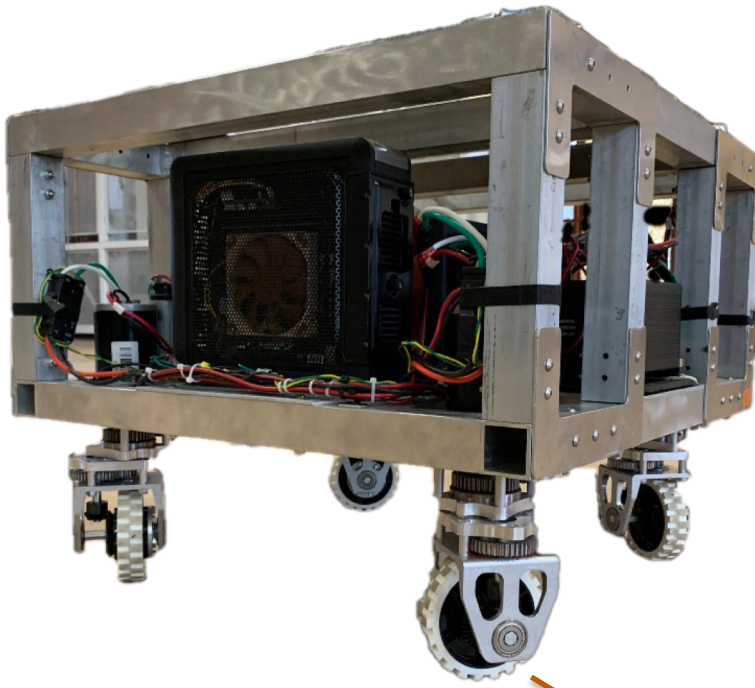


NUCLEAR AND APPLIED ROBOTICS GROUP

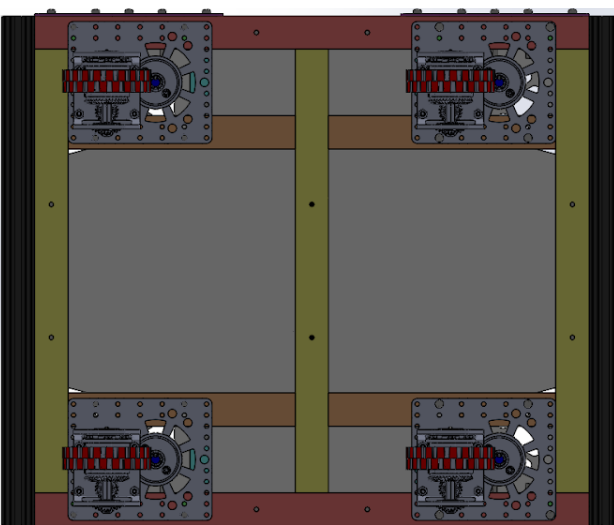
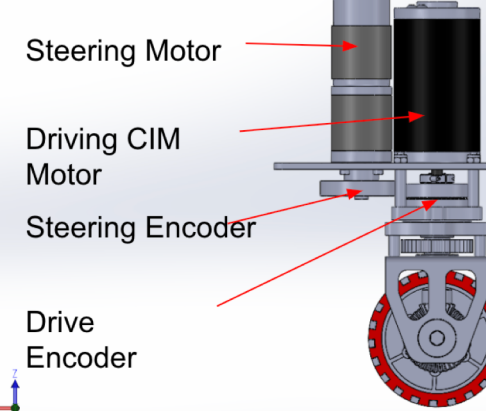
PART 1 : CONTROL

INSTANTANEOUS CENTER OF ROTATION-BASED MASTER-SLAVE KINEMATIC MODELING AND CONTROL

* As presented at 2019 ASME Dynamic Systems and Control Conference [1]



ACTIVE CENTERED CONVENTIONAL WHEEL
MODULE (SWERVE STEER MODULE)



Our Wheeled Mobile Robot Hardware

- Rectangular Aluminum Frame (23''x28'')
- Built to assist with alpha radiation contamination surveys at Los Alamos National Laboratory.
- Non-holonomic
- Pseudo-omnidirectional
- Conventional wheels are subject to less vertical chatter and can carry more load than non-conventional omni wheels.

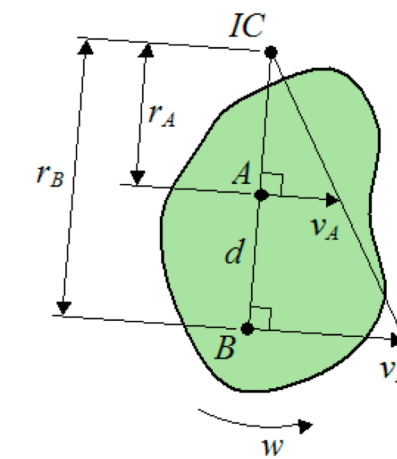
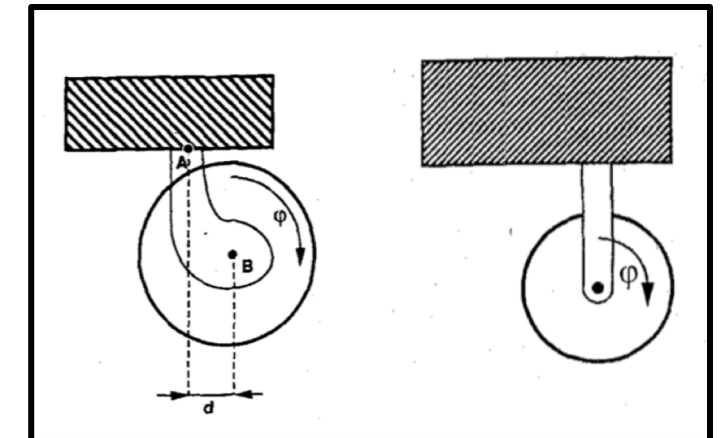


Background

- Centered Orientable Conventional (COC) wheels have singular wheel Jacobians.
- "Soluble motion criterion" is not satisfied, so the actuated inverse solution proposed in seminal work by Muir and Neuman [2] **cannot** be used

Instantaneous Center of Rotation (ICR)

- Point in the robot's plane of motion about which the robot instantaneously rotates about.
- Any admissible wheel configuration can be uniquely identified by the coordinates of its associated ICR [3]
- Singularities:
 - Pure translation
 - ICR located at wheel center
- Artificial Potential Fields [4] and mapping the ICR to spherical coordinates [5] have been proposed to avoid these singularities



Proposed Kinematic Model

$$\mathbf{x} = \begin{bmatrix} x_{ICR} \\ y_{ICR} \end{bmatrix} = \begin{bmatrix} x_r - \dot{y}_r/\omega \\ y_r + \dot{x}_r/\omega \end{bmatrix} \quad (1)$$

$${}^0\dot{\mathbf{e}} = \boldsymbol{\omega} \begin{bmatrix} -y_p \\ x_p \end{bmatrix} \quad (2)$$

$${}^0\dot{\mathbf{m}}_i = \boldsymbol{\omega} \begin{bmatrix} -m_{i_y} + y_{ICR} \\ m_{i_x} - x_{ICR} \end{bmatrix} \quad (3)$$

$${}^0\mathbf{m}_i = \begin{bmatrix} m_{i_x} \\ m_{i_y} \end{bmatrix} = \begin{bmatrix} x_r \\ y_r \end{bmatrix} + \begin{bmatrix} \cos(\theta) & -\sin(\theta) \\ \sin(\theta) & \cos(\theta) \end{bmatrix} {}^R\mathbf{m}_i \quad (4)$$

WMR x, y velocities

$$\dot{x}_r = f(\theta, \omega, \dot{m}_{1_x}) = \frac{-W}{2}\omega\sin(\theta) + \frac{L}{2}\omega\cos(\theta) + \dot{m}_{1_x} \quad (9)$$

$$\dot{y}_r = f(\theta, \omega, \dot{m}_{1_y}) = \frac{W}{2}\omega\cos(\theta) + \frac{L}{2}\omega\sin(\theta) + \dot{m}_{1_y} \quad (10)$$

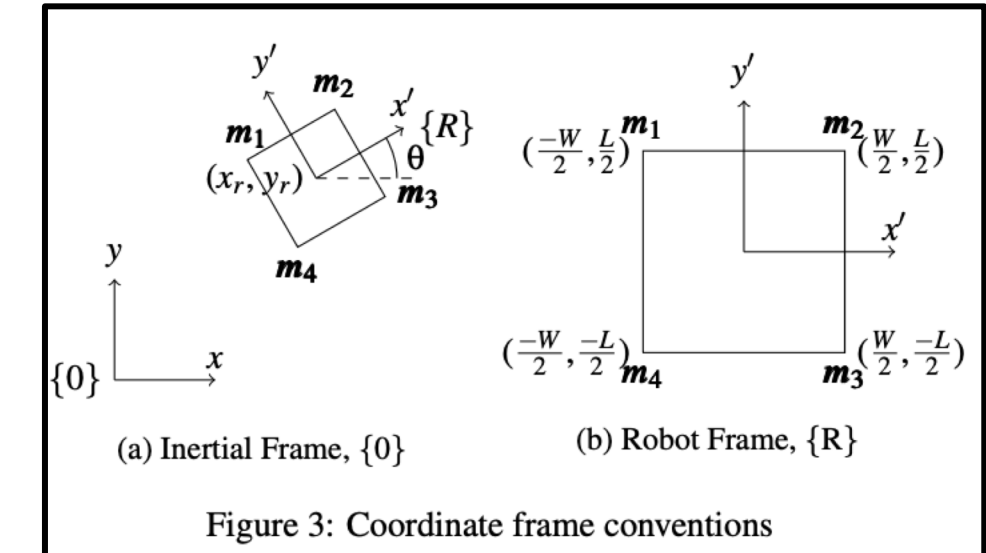


Figure 3: Coordinate frame conventions

- $\omega=0$ singularity avoided
- “ICR on wheel center” singularity eliminated by avoiding ICR control all together; instead, we will control WMR x,y velocities derived from the ICR.

Controllability Analysis

$$\mathbf{x} \equiv \begin{bmatrix} x_1 \\ x_2 \\ x_3 \end{bmatrix} \equiv \begin{bmatrix} x_r \\ y_r \\ \theta \end{bmatrix}, \quad \mathbf{u} \equiv \begin{bmatrix} u_1 \\ u_2 \\ u_3 \end{bmatrix} \equiv \begin{bmatrix} \dot{m}_{1_x} \\ \dot{m}_{1_y} \\ \omega \end{bmatrix}, \quad \mathbf{y} \equiv \mathbf{x} \quad (13)$$

$$\mathbf{C} = [\mathbf{g}_1 \quad \mathbf{g}_2 \quad \mathbf{g}_3 \quad [\mathbf{g}_1, \mathbf{g}_2] \quad [\mathbf{g}_1, \mathbf{g}_3] \\ [\mathbf{g}_2, \mathbf{g}_3] \quad [\mathbf{g}_1, [\mathbf{g}_1, \mathbf{g}_2]] \quad [\mathbf{g}_1, [\mathbf{g}_1, \mathbf{g}_3]] \quad [\mathbf{g}_2, [\mathbf{g}_2, \mathbf{g}_3]]] \quad (16)$$

$$\begin{bmatrix} \dot{x}_1 \\ \dot{x}_2 \\ \dot{x}_3 \end{bmatrix} = \begin{bmatrix} 1 \\ 0 \\ 0 \end{bmatrix} u_1 + \begin{bmatrix} 0 \\ 1 \\ 0 \end{bmatrix} u_2 + \begin{bmatrix} -\frac{w}{2} \sin x_3 + \frac{L}{2} \cos x_3 \\ \frac{w}{2} \cos x_3 + \frac{L}{2} \sin x_3 \\ 1 \end{bmatrix} u_3 \\ \equiv \mathbf{g}_1 u_1 + \mathbf{g}_2 u_2 + \mathbf{g}_3 u_3 \quad (14)$$

$$\mathbf{C} = \begin{bmatrix} 1 & 0 & -\frac{w}{2} \sin x_3 + \frac{L}{2} \cos x_3 & 0 & 0 & 0 & 0 & 0 \\ 0 & 1 & \frac{w}{2} \cos x_3 + \frac{L}{2} \sin x_3 & 0 & 0 & 0 & 0 & 0 \\ 0 & 0 & 1 & 0 & 0 & 0 & 0 & 0 \end{bmatrix} \quad (19)$$

$$rank(\mathbf{C}) = 3$$

Nonlinear, driftless, input-affine system

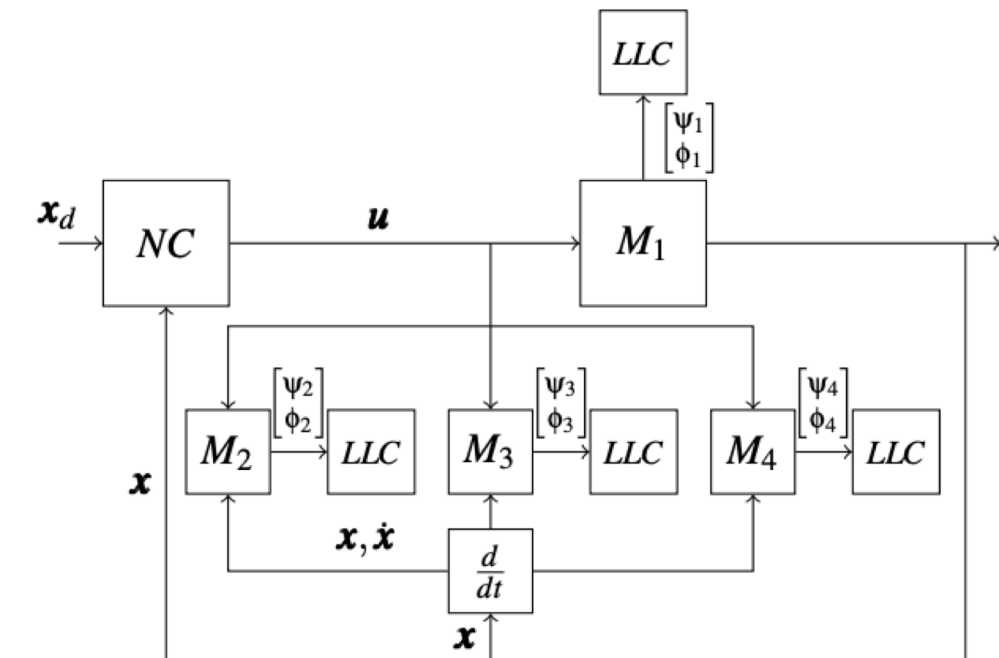
$$\dot{\mathbf{x}} = \mathbf{f}(\mathbf{x}) + \sum_{i=1}^m \mathbf{g}_i(\mathbf{x}) u_i \quad (15)$$

Per Hedrick [7], the system is controllable.

∴ Master wheel can theoretically be controlled to yield any desired position and orientation of the mobile platform.

Control Structure

- NC: any model-based nonlinear controller
 - M_i : kinematic model of the i th wheel module
 - LLC: Low-level controller
 - “Master” wheel: Wheel module chosen for model-based control.
 - “Slave” wheels: Remaining wheels coordinate their steer angles and drive speeds so their drive axes coincide with the ICR (by nature of their kinematic model)
 - Extensible to all platform geometries with n -wheels
 - Steer speeds are assumed to be sufficiently high relative to drive speeds



Feedback Linearization Approach

$$\dot{\mathbf{x}} = \mathbf{G}\mathbf{u} \quad (20)$$

$$\mathbf{u} = \mathbf{G}^{-1}\tilde{\mathbf{u}} \quad (21)$$

Since $\det(\mathbf{G}) \neq 0 \forall x_3 \in \mathbb{R}$, \mathbf{G} is globally invertible, so the control law is globally defined.

Inner-loop P control:

$$\dot{\mathbf{x}} = \tilde{\mathbf{u}} \quad (22)$$

$$\tilde{\mathbf{u}} = k_p(\mathbf{x}_d - \mathbf{x}) \quad (23)$$

Formal bounds on k_p given actuator saturation limits.

$$k_p \leq \sqrt{\frac{(r\psi_{max})^2}{(0.5\Delta x_3 + \Delta x_1)^2 + (0.5\Delta x_3 + \Delta x_2)^2}}$$

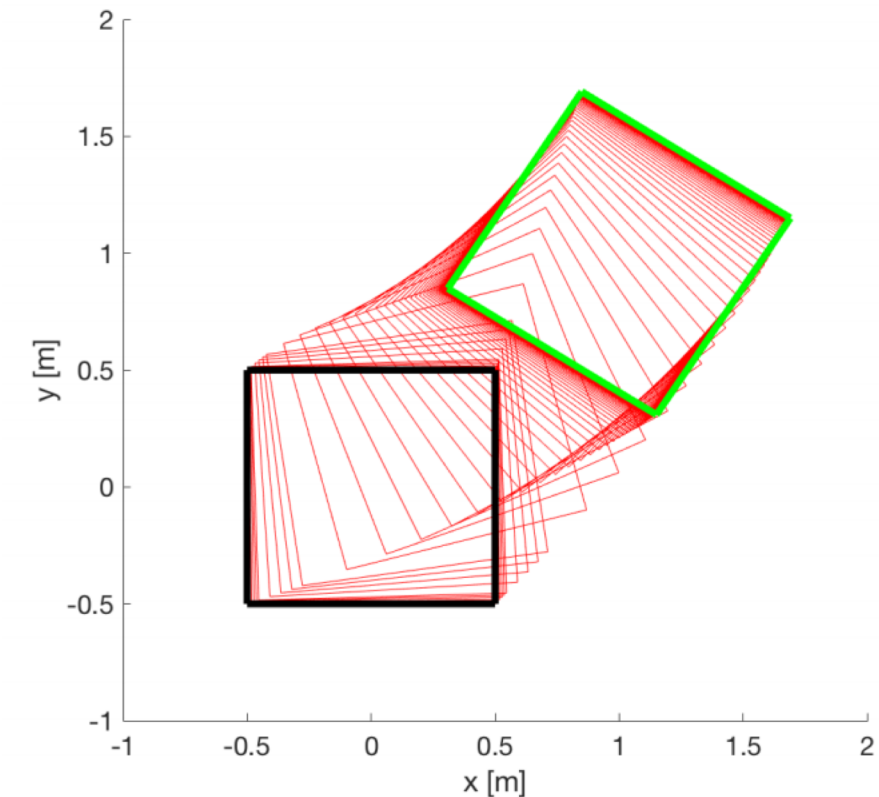


Figure 5: WMR motion in $\{0\}$ frame

Adding Velocity Tracking

- Here, we simply add velocity as a feedforward signal for more accurate tracking and to smooth out trajectories

$$\dot{\mathbf{x}} = \mathbf{Gu} \quad (20)$$

$$\mathbf{u} = \mathbf{G}^{-1}\tilde{\mathbf{u}} \quad (21)$$

$$\dot{\mathbf{x}} = \tilde{\mathbf{u}} + \mathbf{v}_d \quad (22)$$

Plots

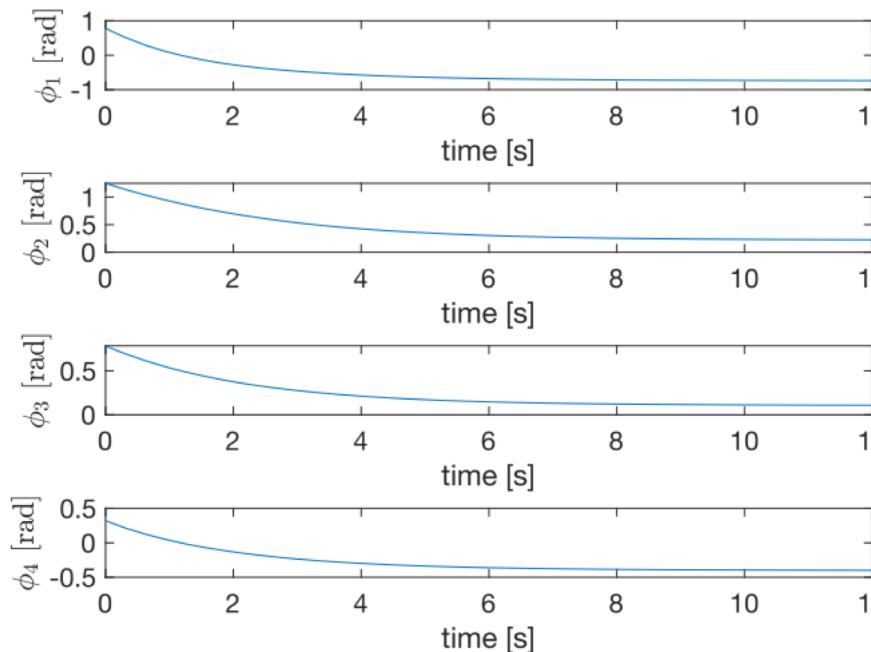


Figure 7: Steer angles for each wheel module

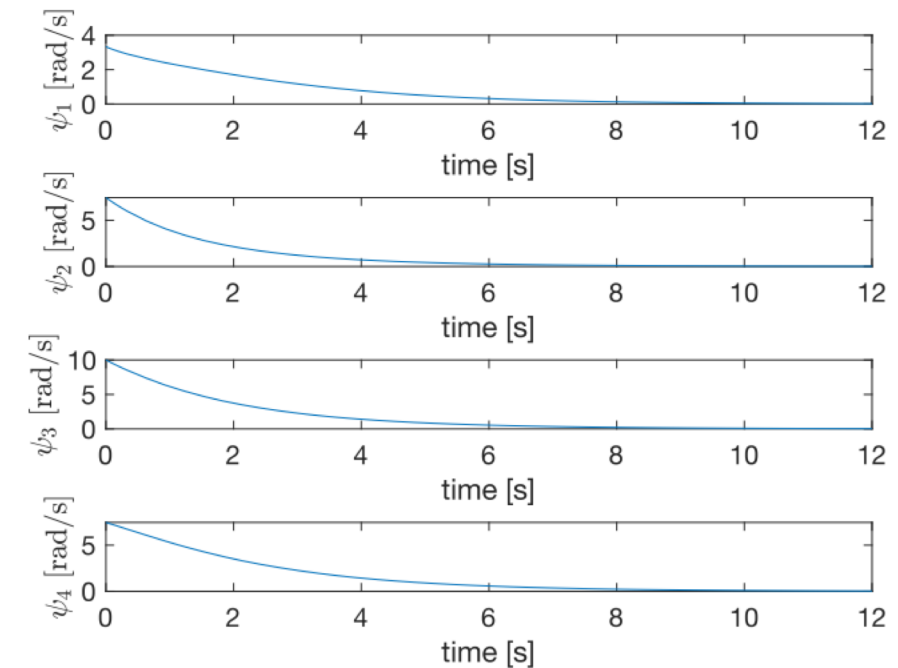


Figure 6: Drive speeds for each wheel module

Plots

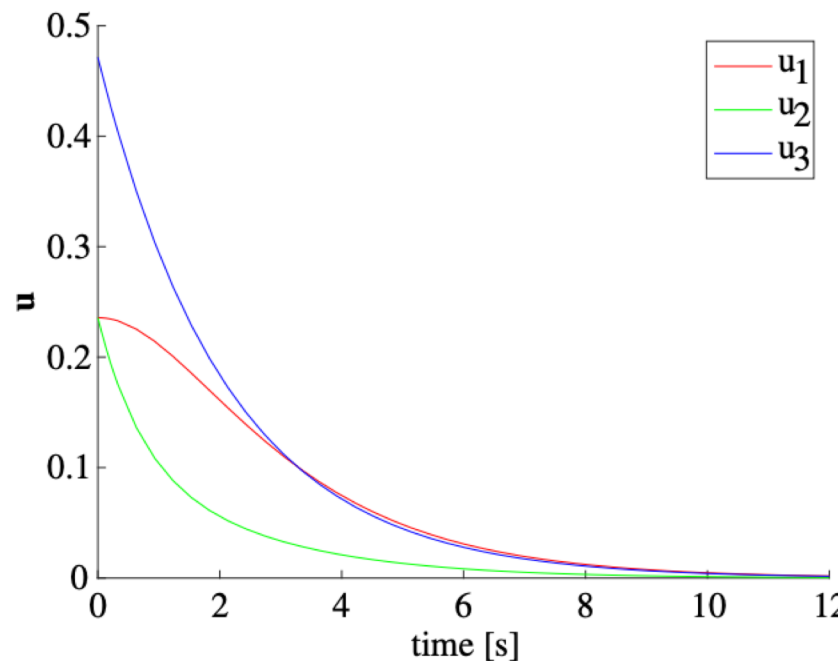


Figure 9: Control input from feedback linearization

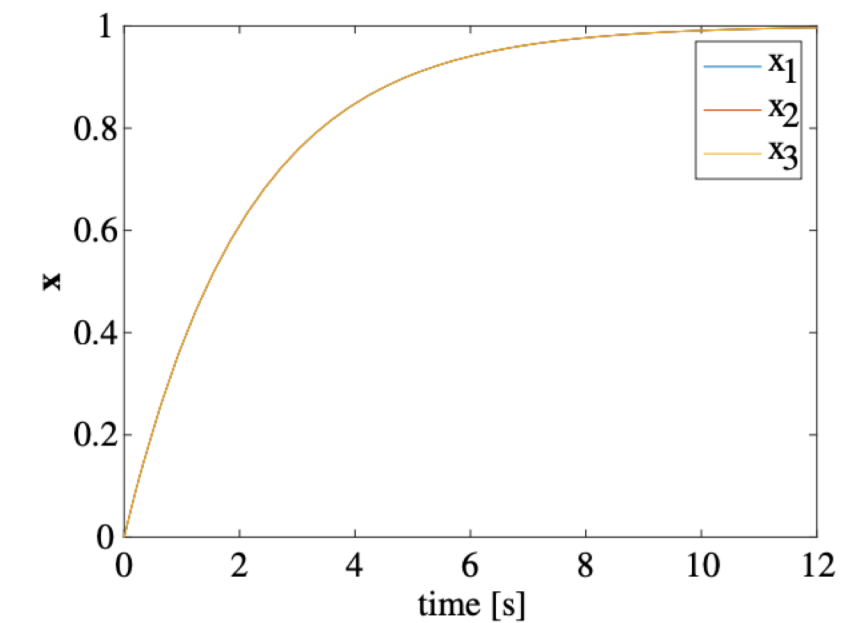


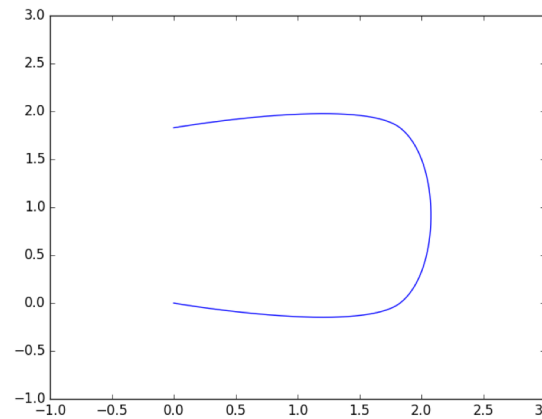
Figure 8: State, \mathbf{x} , response in 12 s time interval. x_1, x_2 , and x_3 share the same time response

Trajectory Generation

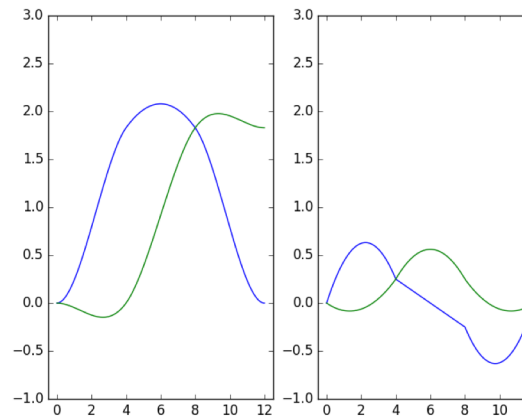
- Polynomial Via Point Trajectories [7]
 - Input: **Via Points (pose, vel, times)**

$$([(x, y, \theta)_1, (x, y, \theta)_2, \dots], [(v_x, v_y, \omega)_1, (v_x, v_y, \omega)_2, \dots], [t_0, t_1, \dots])$$

- Output: Continuous Cubic Trajectory



Trajectory



(a) Position (b) Velocity

Solving for Polynomial

$$\beta(T_j + \Delta t) = a_{j0} + a_{j1}\Delta t + a_{j2}\Delta t^2 + a_{j3}\Delta t^3$$

$$\beta(T_j) = \beta_j, \quad \dot{\beta}(T_j) = \dot{\beta}_j,$$

$$\beta(T_j + \Delta T_j) = \beta_{j+1}, \quad \dot{\beta}(T_j + \Delta T_j) = \dot{\beta}_{j+1}.$$

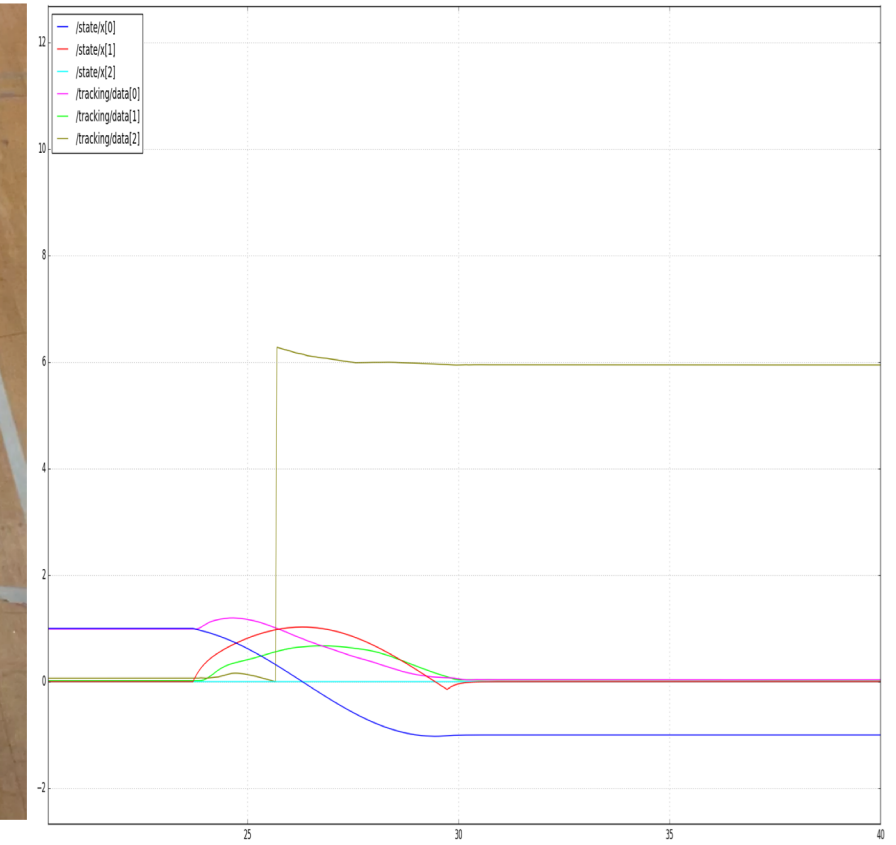
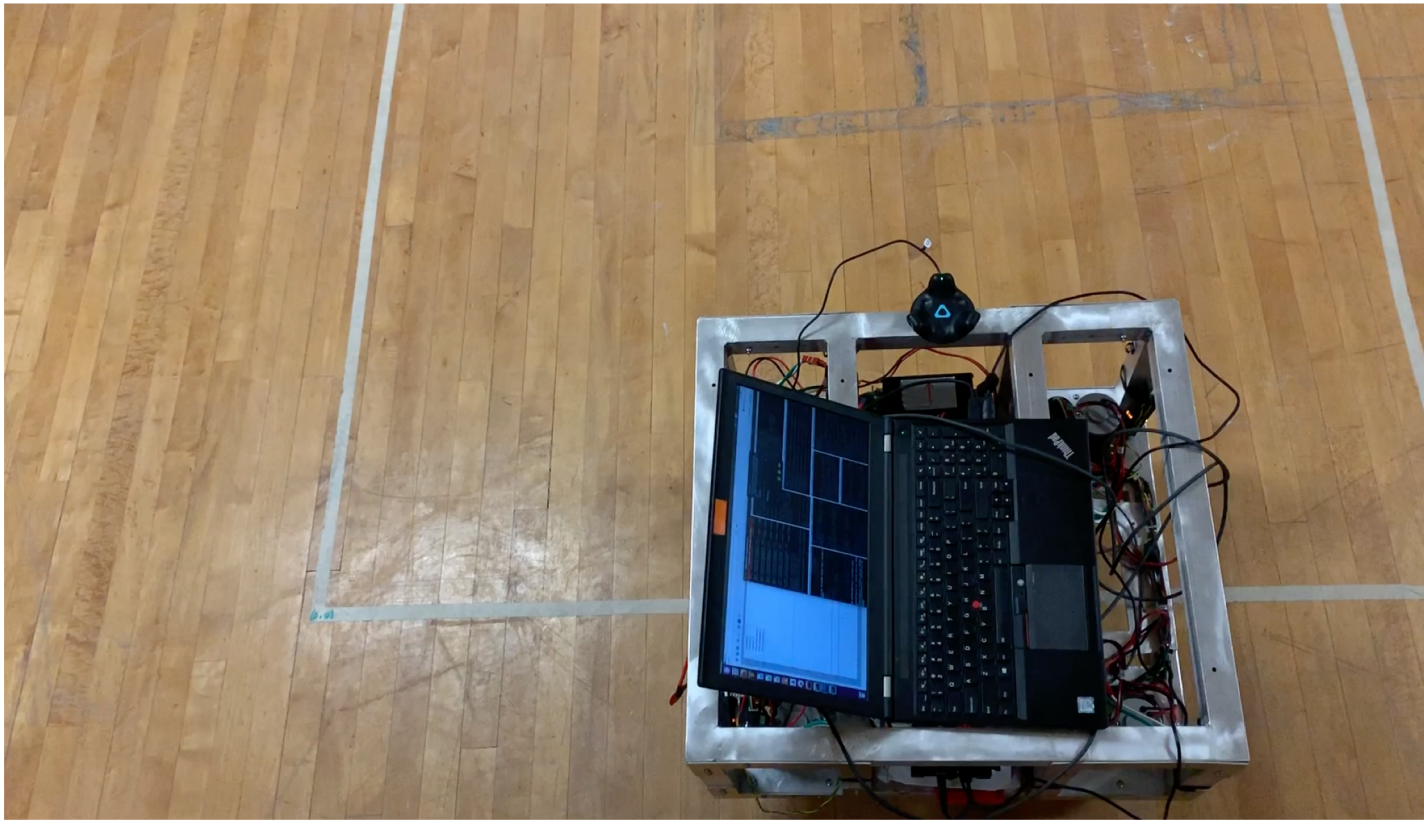
$$a_{j0} = \beta_j,$$

$$a_{j1} = \dot{\beta}_j,$$

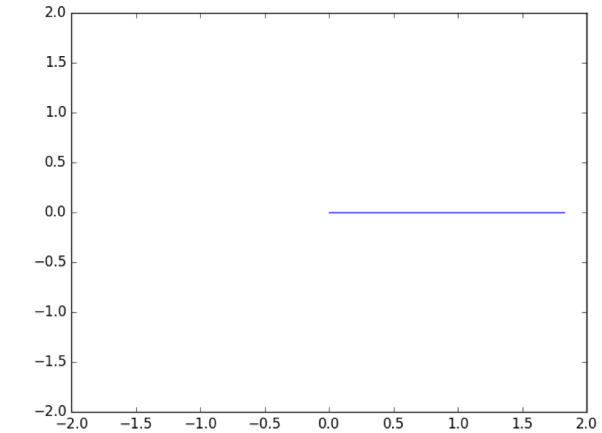
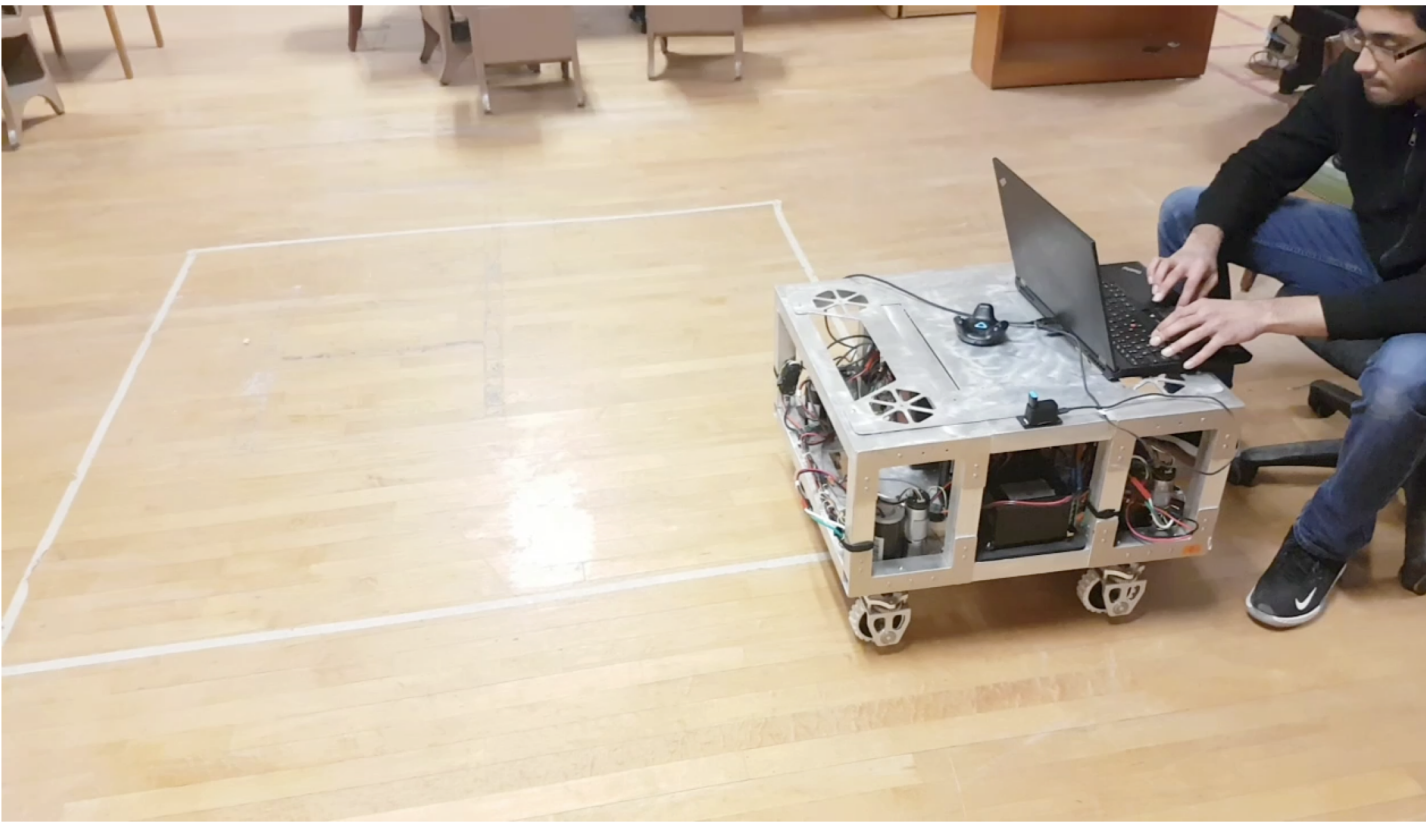
$$a_{j2} = \frac{3\beta_{j+1} - 3\beta_j - 2\dot{\beta}_j \Delta T_j - \dot{\beta}_{j+1} \Delta T_j}{\Delta T_j^2},$$

$$a_{j3} = \frac{2\beta_j + (\dot{\beta}_j + \dot{\beta}_{j+1})\Delta T_j - 2\beta_{j+1}}{\Delta T_j^3}.$$

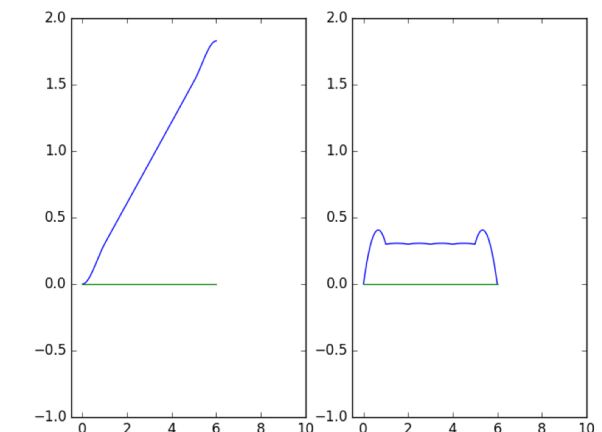
First open-loop test on hardware



Straight line with 180° orientation change

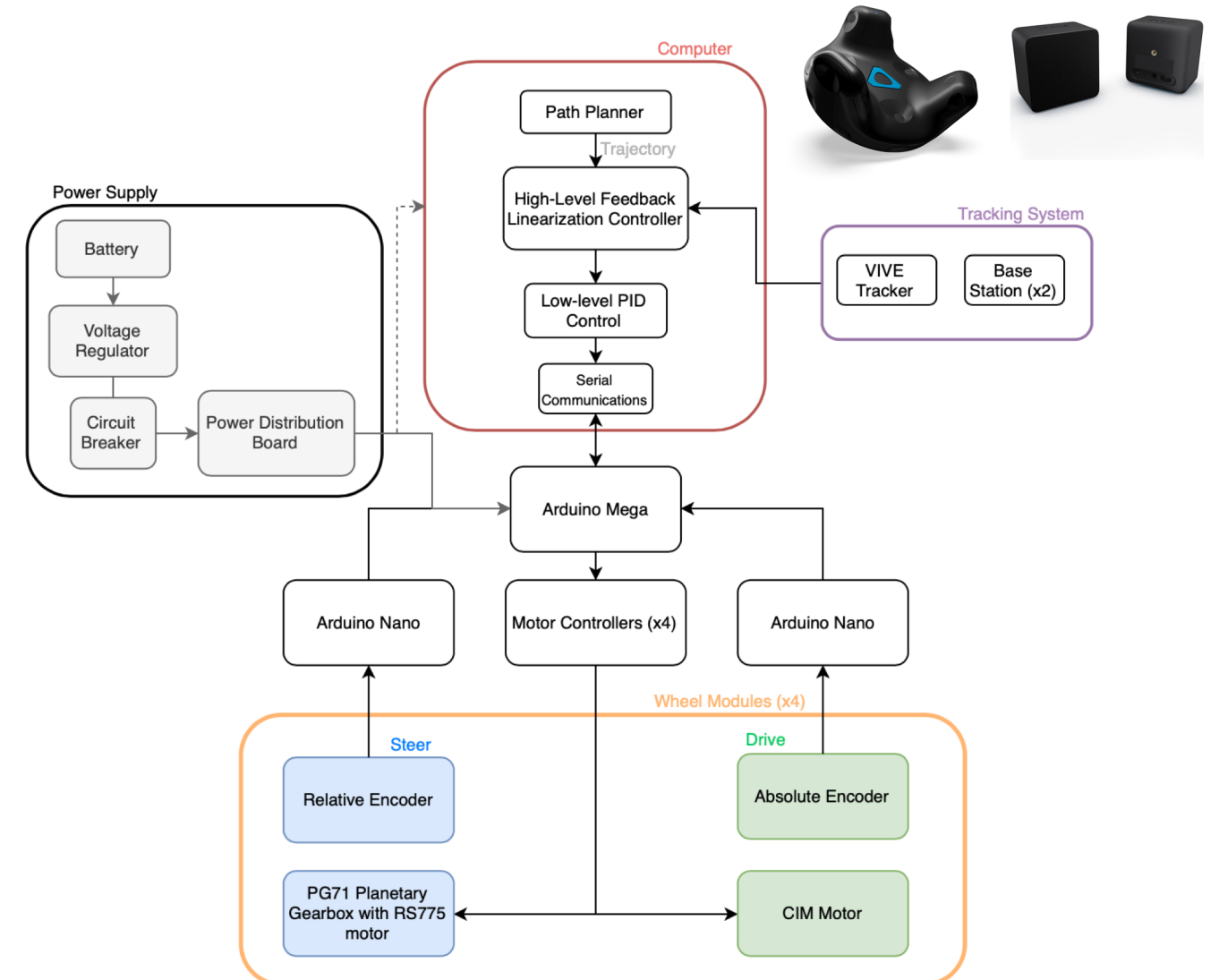


Trajectory



Overview of Architecture

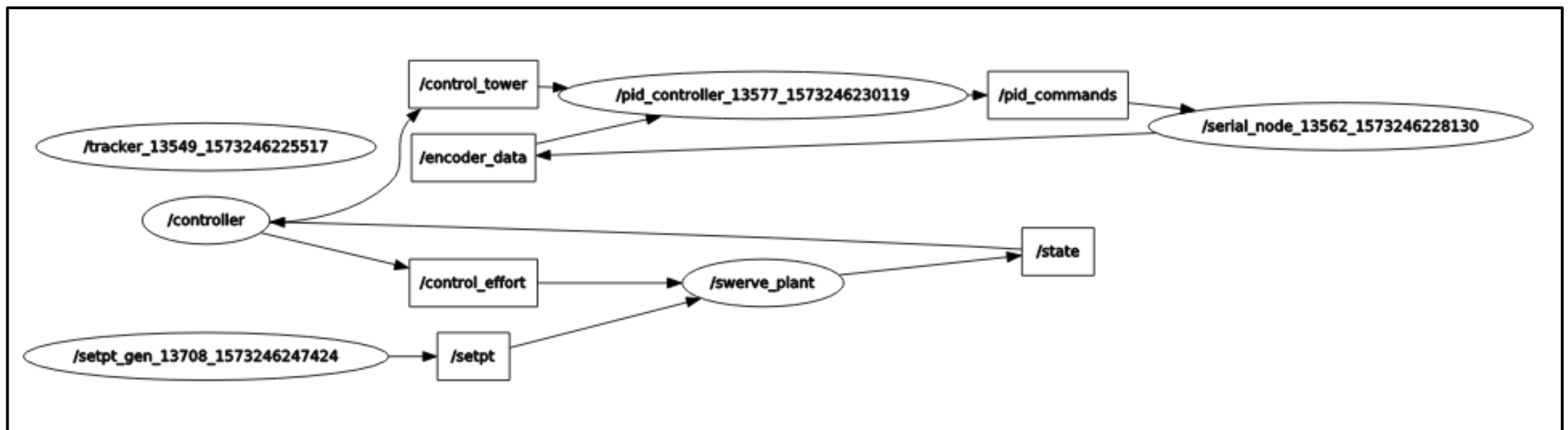
- Hardware is powered by a 24V Battery
- Arduino Microprocessors are used to:
 - Administer Drive Commands
 - Receive Encoder Data
- Computer runs high-level and low-level controllers
- HTC VIVE Trackers used for position, orientation and velocity updates



Software Architecture

- Original theoretical work done using MATLAB and Python
- Programmed the controls algorithm on the robot in Python and C++ using the Robot Operating System (ROS) framework
- Tracker data was obtained by using the OpenVR API
- To calibrate the tracker, we solve a simple Linear Program (LP)

ROS GRAPH (open-loop)



PART 2 : PLANNING

OPTIMAL PATH PLANNING GIVEN A DESIRED OFFSET SENSOR TRAJECTORY

Path Planning using Non-Linear Model Predictive Control (NL MPC)

- Needed to design an algorithm to plan a path for the robot given a desired offset trajectory for its alpha sensor

NL MPC Problem Formulation:

- Robot kinematics modeled as a single integrator, $\dot{x} = u$
- Quadratic Inequality Constraint for Obstacle Avoidance

$$(R_o + R_s + \epsilon)^2 - (x_s - x_o)^2 - (y_s - y_o)^2 \leq 0$$

- Nonlinear Coordinate Transformation

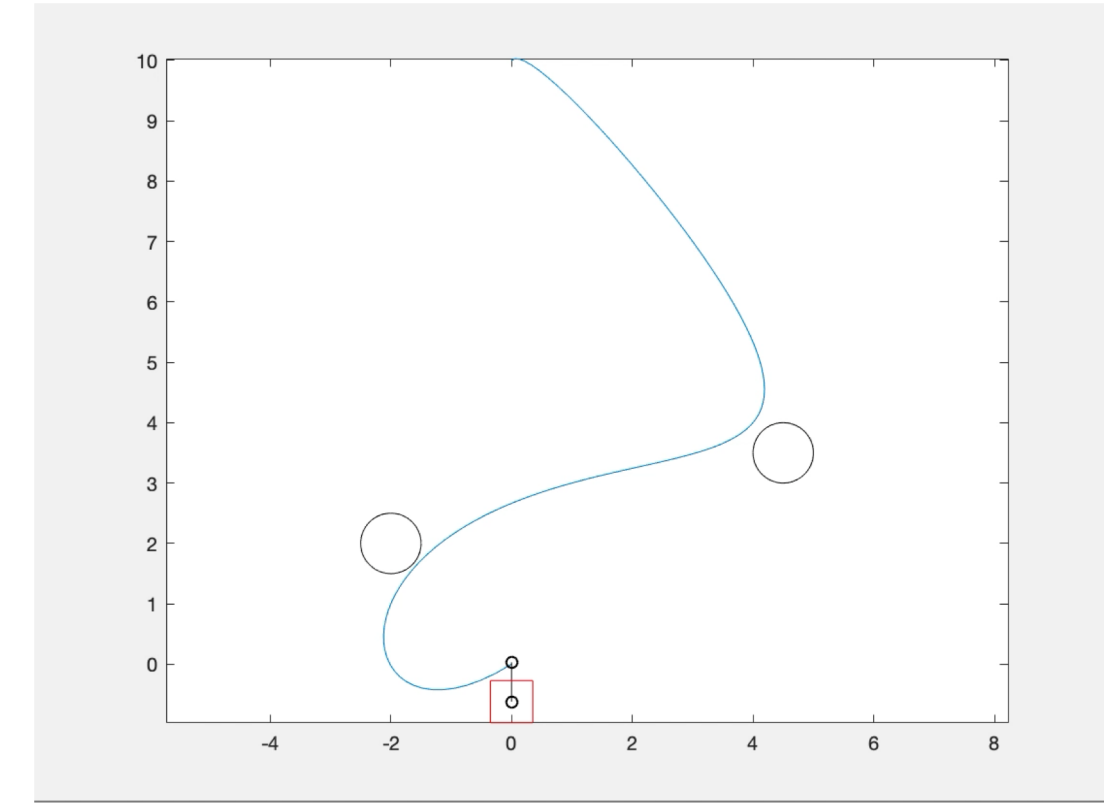
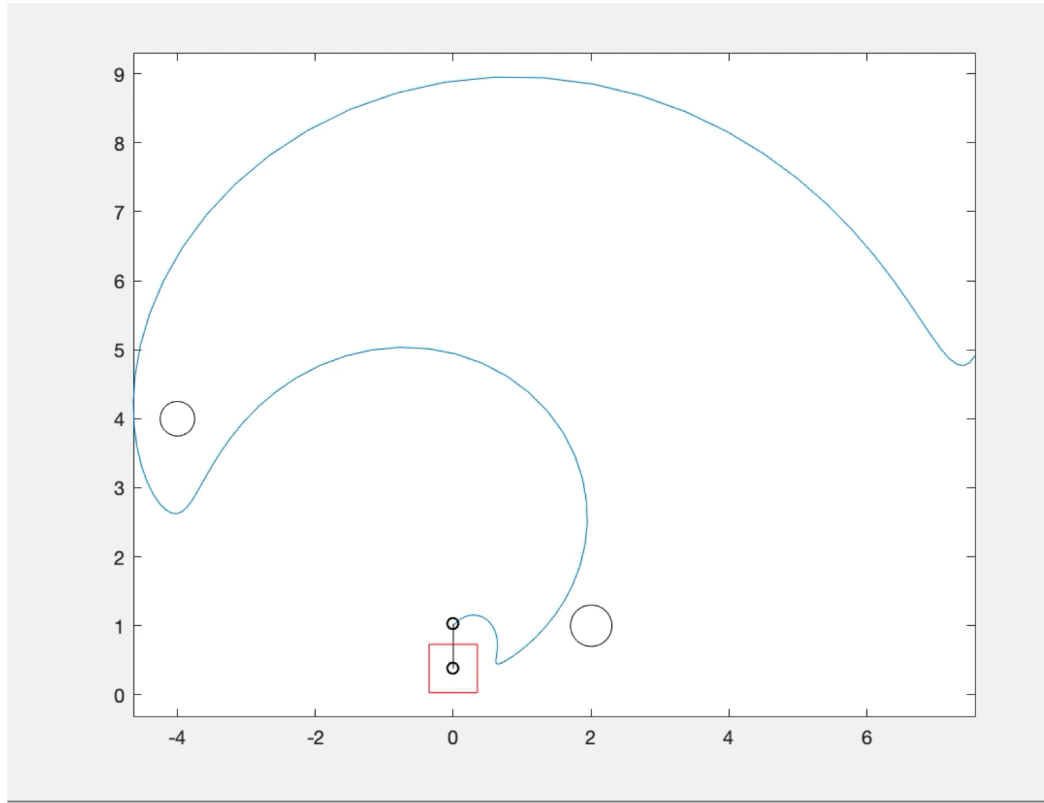
$$\begin{aligned} x_{alpha}(t) &= X(t) - L * \cos(\theta) \\ y_{alpha}(t) &= Y(t) - L * \sin(\theta) \end{aligned} \quad p_{alpha} = \begin{bmatrix} x_{alpha} \\ y_{alpha} \end{bmatrix}$$

- Quadratic Cost

$$l(x(t), u(t)) = p_{alpha}(t)^T Q p_{alpha}(t) + u(t)^T R u(t), Q \succeq 0, R \succeq 0$$

- Solved this constrained nonlinear optimization problem using Sequential Quadratic Programming (SQP)

Path Planning using Non-Linear Model Predictive Control (NL MPC)



Future Work

- Eliminate Nonlinearity in MPC formulation by
 1. Using a piecewise approximation of \sin and \cos in the coordinate transformation
 2. Setting binary decision variables to decide which piece to use
 3. Formulate a Mixed Integer Quadratically Constrained Quadratic Program (MIQCQP) which will allow for
 1. Faster computation times
 2. Less risk of getting stuck in a local minima
- Coverage Path Planning (CPP) algorithms for the robot
- Improving existing hardware by redesigning the wheel modules

Thank you!
Questions?

References

- [1] Ramanathan, Vikram, Zelenak, Andy, and Pryor, Mitch. "Instantaneous Center of Rotation-Based Master-Slave Kinematic Modeling and Control." *Proceedings of the ASME 2019 Dynamic Systems and Control Conference. Volume 3, Rapid Fire Interactive Presentations: Advances in Control Systems; Advances in Robotics and Mechatronics; Automotive and Transportation Systems; Motion Planning and Trajectory Tracking; Soft Mechatronic Actuators and Sensors; Unmanned Ground and Aerial Vehicles.* Park City, Utah, USA. October 8–11, 2019. V003T17A005. ASME. <https://doi.org/10.1115/DSCC2019-9123>
- [2] Muir, P. F., and Neuman, C. P., 1990. Autonomous Robot Vehicles. Springer New York, New York, NY.
- [3] Thuilot, B., d'Aandrea-Novel, B., and Micaelli, A., 1996. "Modeling and feedback control of mobile robots equipped with several steering wheels". *IEEE Transactions on Robotics and Automation*, 12(3), June, pp. 375–390.
- [4] Dietrich, A., Wimbock, T., Albu-Schaffer, A., and Hirzinger, G., 2011. "Singularity avoidance for nonholonomic, omnidirectional wheeled mobile platforms with variable footprint". In *2011 IEEE International Conference on Robotics and Automation*, pp. 6136–6142.
- [5] Connette, C. P., Pott, A., Hagele, M., and Verl, A., 2008. "Control of an pseudo-omnidirectional, non-holonomic, mobile robot based on an icm representation in spherical coordinates". In *2008 47th IEEE Conference on Decision and Control*, pp. 4976–4983.
- [6] Kulkarni, A., 2009. "Instant center based kinematic and dynamic motion synthesis for planar mobile platforms". PhD thesis, Univ. of Texas at Austin, Austin, Texas.
- [7] Hedrick, J. K., and Girard, A., 2010. Control of Nonlinear Dynamic Systems: Theory and Applications. Self-published.
- [8] Park, Frank C., and Lynch, Kevin M.. Modern Robotics: Mechanics, Planning, and Control. United Kingdom, Cambridge University Press, 2017.